ASME©

This manuscript version is made available under CC-BY licence.

IMPORTANCE OF 3D VEHICLE HEAT EXCHANGER MODELING

Ing. Michal Schmid[1], prof. Ing. Petr Paščenko, Ph.D.[2], Ing. Fatih Bozkurt[3], Ing. Pavel Petržela[4]

[1]University of Pardubice, Faculty of Transport Engineering, Pardubice, Czechia, michal.schmid3@gmail.com

[2]University of Pardubice, Faculty of Transport Engineering, Pardubice, Czechia, Petr.Pascenko@upce.cz

[3]Vocational School of Transportation, Eskisehir Technical University, Eskisehir, Turkey, fatihbozkurt@eskisehir.edu.tr

[4]SVOS s.r.o, Prelouč, Czechia, petrzela@armsvos.cz

Key words: 3D and 1D CFD, Heat Exchanger, Temperature Prediction Accuracy, Uniformity Index, Primary and Auxiliary Fluid

ABSTRACT

The work demonstrates, via a comprehensive study, the necessity of using a 3D CFD approach for heat exchanger (HTX) modelling within underhood vehicle simulation. The results are presented as the difference between 1D and 3D CFD approaches with a focus on auxiliary fluid (e.g. coolant) temperature prediction as a function of primary fluid (e.g. air) inlet conditions. It has been shown that the 1D approach could significantly underpredict auxiliary fluid inlet temperature due to neglecting the spatial distribution of primary fluid velocity magnitude. The resultant difference in the auxiliary fluid flow HTX inlet temperature is presented and discussed as a function of the Uniformity Index (UI) of the primary fluid flow velocity magnitude. Additionally, the 3D HTX model's importance is demonstrated in an industrial example of full 3D underhood simulation.

INTRODUCTION

Nowadays, so-called underhood thermal management (UHTM) 3D CFD simulation is an inherent part of modern vehicle development. Within all the modern vehicles there are implemented variety of heat exchangers (HTXs) and the cooling air source differs between industrial applications or even within a vehicle load case. Typically, the most challenging situation for vehicle thermal management occurs when the cooling air flow is produced only via a fan in combination with the peak power dissipation into the system. Nevertheless, this condition occurs seldom for conventional passenger cars. On the other hand, it is very likely for application in other industries such as defence vehicles, buses, excavators, loaders, agricultural vehicles, static diesel generators, motorsport applications, etc. It is the worst-case scenario due to zero vehicle speed (no ram air) and in addition, due to low air flow uniformity on the HTX air inlet. From the perspective of UHTM simulation, the key outcome is cooling air temperature, flow and HTX interior fluid temperature (e.g. of coolant, transmission oil, etc.). As the prediction of HTX interior fluid inlet/outlet temperature is crucial from a thermal engineering point of view, the presented study focuses on HTX interior fluid temperature prediction modelling.

The scheme in Figure 1 shows a passenger car under bonnet area cross-section. Cooling pack HTXs and a simplified air flow path are displayed within the figure [1].
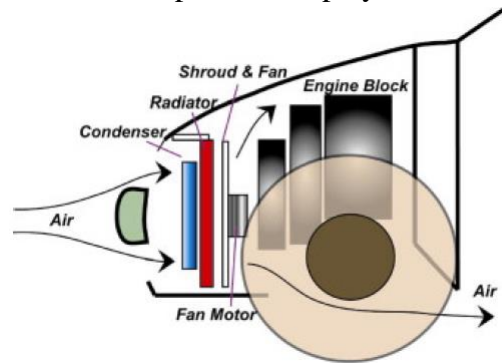
Figure 1. Schematic Underhood [1]

The necessity of 3D CFD for accurate prediction of the primary side is comprehensively discussed in [1-3], additionally under transient conditions in [4,5]. 3D CFD underhood simulation is currently a common part of virtual vehicle development, including wind tunnel geometry [6]. The importance of 3D CFD underhood simulation correspondingly for other systems (not only the cooling pack) is part of current research as well. For example, accessory units' implementation [8], a passenger car aerodynamic drag coefficient [9], or connecting with ICE engine modelling [10]. Additionally, full thermal vehicle model contains other heat transfer phenomena like natural convection or radiation [11]. Accurate underhood simulation provides for the components' thermal models valid boundary or initial conditions [8,11]. Regarding HTX simulation, the full 3D approach takes into account HTX air inlet spatial conditions and auxiliary (coolant) flow direction in contrast to the 1D method, where total or average values take place. The use of a predicted total air mass flow rate and average inlet temperature (1D approach) simulation is a generally valid approach with reasonable accuracy. However, one could imagine a scenario where this could lead to misleading prediction. An extreme case demonstrates the scenario with underpredicted coolant inlet temperature via the 1D approach: A sufficient total air mass flow rate is produced by the cooling system from a 1D point of view, however only throughout a small region of the HTX frontal area. This system would be judged via the 1D approach as sufficient; however, the coolant temperature will in reality be above the required temperature target. This is crucial as required prediction accuracy is in units of degrees Celsius or may even be lower in low heat dissipation HTXs typical for modern electric vehicles.

Within the paper, the 3D HTX model is implemented in GNU Octave 5.2.0 and compared with the commercial tools ANSYS Fluent and Siemens STAR-CCM+, with the aim of verifying the implementation and assessing the model. The model is further used for a study focused on HTX core fluid inlet temperature prediction as a function of cooling air inlet conditions. The study conducted demonstrates the necessity of using the 3D model rather than 1D, under applied specific conditions. The air fluid and the HTX internal fluids (coolant) are referred within the work as the primary side and the auxiliary side.

1. HEAT EXCHANGER MODEL

HTX core geometry length scale is smaller in order of magnitude compared to a typical vehicle. Direct modelling of a tube and fins complicated geometry in a higher level of detail is not computationally effective. Hence, the HTX core is simplified within the full vehicle 3D

CFD simulations via a porous zone, where the mass transfer is modelled by Darcy's law with appropriate inertia and viscous coefficients [12]. The heat transfer within the porous zone is not directly modelled. The aforementioned length scale difference between the HTX and vehicle is discussed in more detail with a multi-scale modelling approach in [12].

Generally, the types of heat exchangers (HTXs) used in vehicles are so-called cross-flow HTXs as shown in Figure 2 with both fluids unmixed [13].
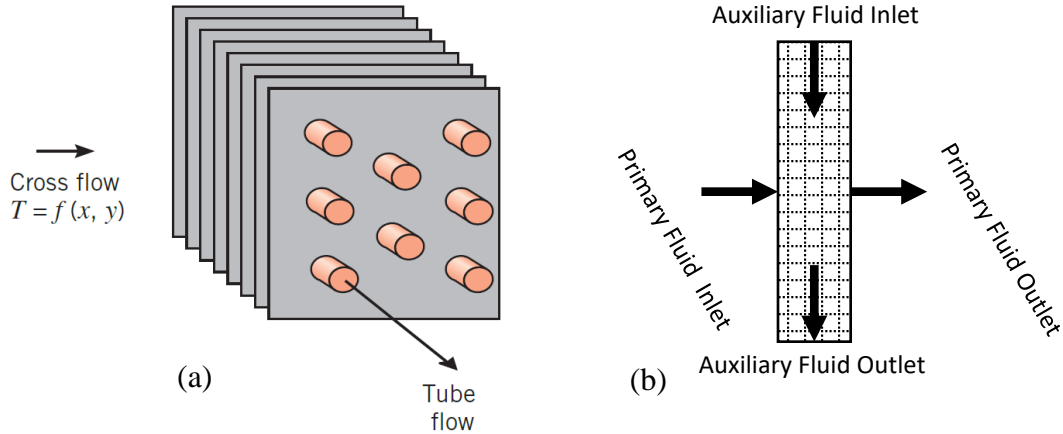
Figure 2. Cross-Flow Heat Exchanger (a) and Flow Nomenclature Scheme (b) [13]

For this type of heat exchangers, the effectiveness-NTU method is typically used to determine the heat transfer and temperature as the log mean temperature approach cannot be used. The HTX model is based on empirical characteristic data provided by a physical measurement (Table 1). The NTU stands for the Number of Transfer Units and is defined as a dimensionless parameter by the expression **(1)** [13-15].

$$NTU = \frac{UA}{C_{min}} \tag{1}$$

Where the U refers to heat transfer coefficient $\left(\frac{W}{m^2 K}\right)$ and the A to heat transfer area (m^2). The minimal heat capacity $C_{min}\left(\frac{W}{K}\right)$ definition is expressed by the equation **(2)**. It represents the minimum from the auxiliary fluid and primary fluid heat capacity, or maximum respectively.

$$C_{min/max} = min/max\{\dot{m}_{auxiliary} c_{p,auxiliary}; \dot{m}_{primary} c_{p,primary}\} \tag{2}$$

The effectiveness is defined as ratio of the actual heat transfer rate and maximum possible heat dissipation (an infinite HTX core length is assumed) **(3)**.

$$\varepsilon = \frac{q}{C_{min}(T_{in,aux} - T_{in,prim})} \tag{3}$$

Relation between the *effectiveness* and the *NTU* is expressed via **(4)**, were the *Cr* is ration of C_{min} and C_{max} as shown in the **(5)**. The expression **(4)** is exactly correct only for $C_r=1$. Nevertheless, it could be used as feasible approximation for $0<C_r<=1$ [13].

$$\varepsilon = 1 - exp\left[-\frac{NTU^{0.22}}{C_r}\left(1 - e^{-C_r NTU^{0.78}}\right)\right] \tag{4}$$

$$C_r = \frac{C_{min}}{C_{max}} \tag{5}$$

The described model is implemented into a 3D CFD code in aim to capturing primary outlet spatial distribution as well as auxiliary inlet and outlet temperature. In general, there are two different approaches: the so-called Macro Based Model and the Dual Cell Model. The two models differ in the approach to auxiliary fluid flow modelling. Both the approaches are

3

equivalent from the study perspective as the study is focused on the heat transfer between the fluids.

1.1 Macro Based Model

The Macro Based Model refers to an approach where the modelling described above is applied to multiple local macros (in the study directly a computational cell) and the heat transfer properties are scaled according to the equation **(6)** [16]. The auxiliary fluid flow is not directly calculated with the CFD model, and uniform distribution is assumed.

$$NTU_{local} = NTU_{global} \frac{V_{local} C_{min,global}}{V_{global} C_{min,local}} \tag{6}$$

The computational cell local heat is then calculated according to the equation **(7)** [15]and the final temperature via energy equation **(8)** [16].

$$q_{local} = \varepsilon_{local} C_{min,global} (T_{inlet,auxiliary} - T_{inlet,primary}) \tag{7}$$

$$q = \dot{m} c_p \Delta T \tag{8}$$

Consequently, there are two ways to define the HTX input, total heat rejection or fixed auxiliary inlet temperature. In the study, the scenario with the fixed heat rejection is used as it is more straightforward for typical vehicle cooling applications, where the heat release should be known and the cooling system's target values are associated with the auxiliary inlet temperature. The whole model is solved iteratively until the prescribed heat release is satisfied and the auxiliary inlet temperature is then the output from the simulation. However, the effectiveness-NTU relation is solved iteratively before the solver initialisation by the Newton-Raphson method as the equation **(4)** cannot be manipulated directly to express NTU as a function of effectiveness **(12)**.

1.2 Dual Cell Model

In order to capture more complex patterns of auxiliary flow fields, an additional computational domain is introduced on the auxiliary flow side in the overlap with the primary-fluid side computational mesh. Within the additional auxiliary fluid computational domain, the flow is directly simulated in contrast to the Macro Based Model. The heat transfer between the cells of the primary side of the heat exchanger and the auxiliary side is modelled by means of the effectiveness-NTU similarly to the above-described Macro Based Model. It should be noted that ANSYS Fluent uses the NTU approach in comparison with an iterative approach of Siemens STAR-CCM+. However, the idea of the Dual Cell approach is the same [16,17].

1.3 Test Case Definition and Verification

The Macro Based Model described above was implemented in GNU Octave 5.2.0. The aim of the implementation is to generate data used in the work and to create a base for developing the model itself. The HTX test case domain evaluated is shown in Figure 3. The coordinate system is defined according to a vehicle's typical global coordinate system [18]. The domain numerical decomposition in the coordinate system axes is (8,70,80), where the basic dimensions and mesh size is given in Figure 3. The flow direction of the auxiliary fluid is the positive z-axis and of the primary fluid the positive x-axis.

$$(|x|; |y|; |z|) = (0.04; 0.7; 0.6)m$$
$$(\Delta x; \Delta y; \Delta z) = (0.005; 0.01; 0.01)m$$
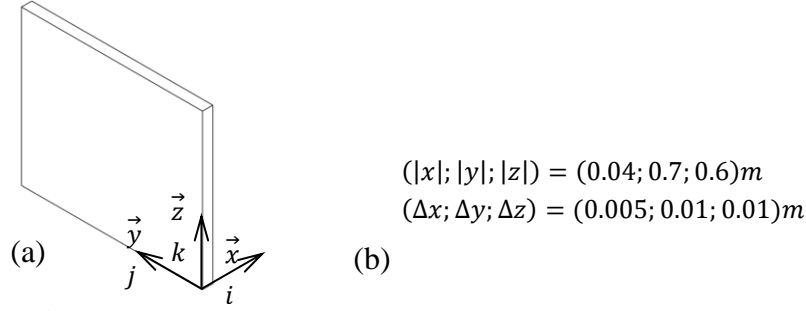
Figure 3. HTX Domain (a) and Domain/Mesh Size (b)

As aforementioned, the analysis focuses on the heat transfer, hence the flow in the test case is inviscid, and no pressure drop throughout the domain is assumed for the sake of simplification. The heat performance characteristic (so-called Q-Table) of the applied HTX is shown below in Table 1.

Table 1. Heat Exchanger Performance Characteristic Data [16]

Heat Rejection [kW]	Coolant Flow [kg/s]		
Air Flow [kg/s]	2.535	3.169	3.803
0.567	26.19	26.64	26.49
0.945	40.89	41.35	41.68
1.512	56.18	57.13	57.79
2.268	70.57	72.14	73.25
3.024	81.53	83.68	85.20
3.780	90.79	93.50	95.43

The implementation of the HTX model was verified by comparison with the commercial tools in two different load cases. The test case simulations were performed with a uniform primary- fluid inlet temperature of 319.15K, HTX heat dissipation of 40.0kW and an auxiliary fluid flow rate of $3.1693 \frac{kg}{s}$. The load cases are selected as only the linear interpolation is performed within the range of the Q-Table to avoid an extrapolation. The auxiliary fluid material properties used are water liquid-like. Specifically: density of $1000 \frac{kg}{m^3}$ and specific heat capacity of $4000 \frac{J}{kgK}$. However, the industry typical cooling liquid is a mixture of water and glycol (so-called coolant) and a coolant circuit is pressurised with the aim of increasing the freezing point, boiling temperature and protecting the solid components from corrosion. The primary fluid is defined by the properties of dry air material at the inlet temperature.

The implementation verification load cases differ in the primary fluid inlet profile. The profiles are highlighted in Figure 4. Profile A refers to a uniform primary- fluid inlet velocity magnitude, while Profile B refers to a sinus function-based velocity profile.

5
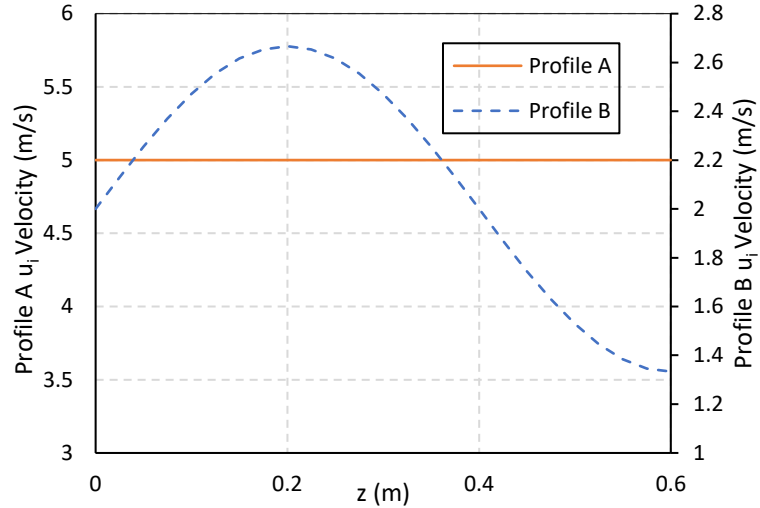
Figure 4. Verification Inlet Profiles

The verification results are summarised in Figure 5. Comparison between GNU Octave 5.2.0. and the commercial tools (ANSYS Fluent and STAR-CCM+) is made via the primary (air) outlet temperature contour and the auxiliary fluid (water) inlet temperature. The 1D auxiliary inlet temperature refers to a value calculated by the steady-state energy equation (8) with the total inlet- air mass flow rate, thus without taking into account the air inlet velocity magnitude spatial distribution. The 3D auxiliary inlet temperature is the area average from the auxiliary inlet cells. It could be observed that the air temperature contour profile as well as the auxiliary inlet temperatures are in good agreement between the CFD codes. Hence, the GNU Octave 5.2.0 implementation is assumed as valid for the next study and future HTX model development.

In addition to the GNU Octave implementation verification, the test case provides information about the difference between 1D and 3D prediction. There is some difference between 1D and 3D model auxiliary inlet temperature prediction, even in the scenario of constant primary inlet velocity magnitude. Nevertheless, the difference is relatively small (below or equal to 0.2K) and could be explained only by an averaging error on the auxiliary fluid side. The difference is discussed in higher level of detail within the chapter below.
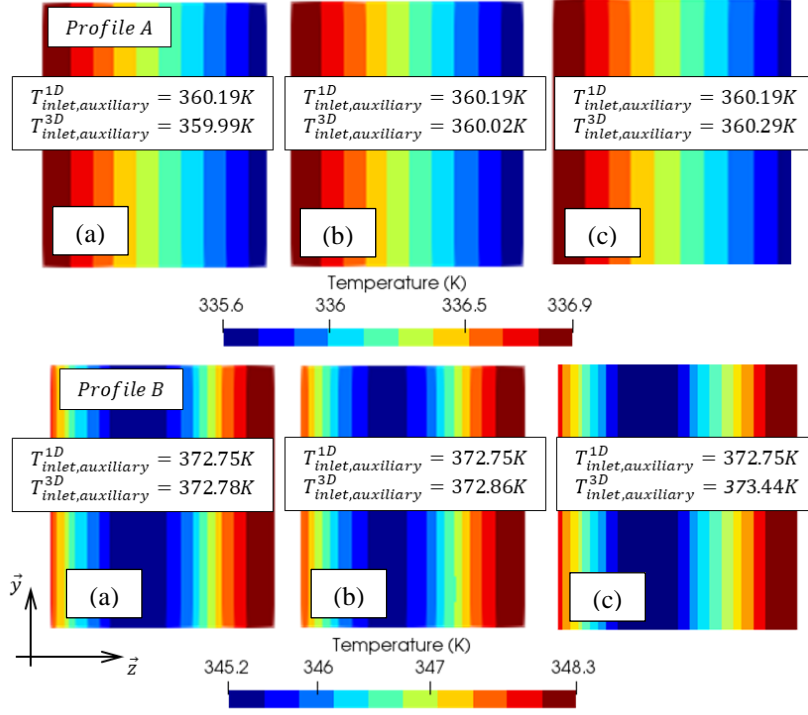
Figure 5. Contour of Air Outlet Temp. for Octave (a), Fluent (b) and STAR-CCM+ (c)

2. STUDY OF AUXILIARY FLUID INLET TEMPERATURE

The study focuses on the primary inlet velocity profile effect on auxiliary inlet temperature prediction. The auxiliary fluid inlet temperature is the key outcome from a UHTM simulation. It compares the difference of prediction between the 1D and 3D approaches, referred to as ΔT. The 1D approach used the total mass flow rate of the primary fluid through the HTX and the described HTX heat transfer model, and the 3D approach used the Macro Based Model. Hence, the 1D approach ignores the spatial distribution of the primary fluid velocity on the HTX inlet. Within the study, the primary inlet (air) temperature is assumed as constant 319.15K. The air inlet temperature is an important parameter affecting the ΔT as well; however, the temperature effect is outside the study scope. The study domain and HTX characteristics are consistent with the test case presented above.

As only the primary fluid velocity profile is assumed, a Uniformity Index (UI) was selected as a key parameter of the study. The UI is defined according to the continuous expression **(9)** [19]and for the computational mesh discretised domain by the expression **(10)**.

$$UI = 1 - \frac{\int |u_i - \bar{u}| \, dA}{2|\bar{u}|A} \tag{9}$$

$$UI = 1 - \frac{\sum_{jk} |u_i - \bar{u}| A_{jk}}{2|\bar{u}| \sum_{jk} A_{jk}} \tag{10}$$

In order to maintain consistent comparison between the study runs, a constant primary inlet mass flow rate of $1.512 \frac{kg}{s}$ is introduced. The UI study was created using a step function for the inlet velocity profile with a variable peak value. With a constant minimal value of $u_i^{min} = 1.23 \frac{m}{s}$, the peak value is varying to satisfy the constant total mass flow rate. In Figure 6 examples of inlet profiles used are shown.

7

The study results are presented as an auxiliary fluid inlet temperature difference between each run and 1D approach (ΔT) as a function of the UI. During the study, the most contributing parameters were identified as the imposed heat into the system and primary fluid inlet profile minimal velocity. In order to demonstrate these effects, the UI study was performed for multiple HTX heat dissipation and primary fluid velocity step function profile with minimum velocity magnitude.
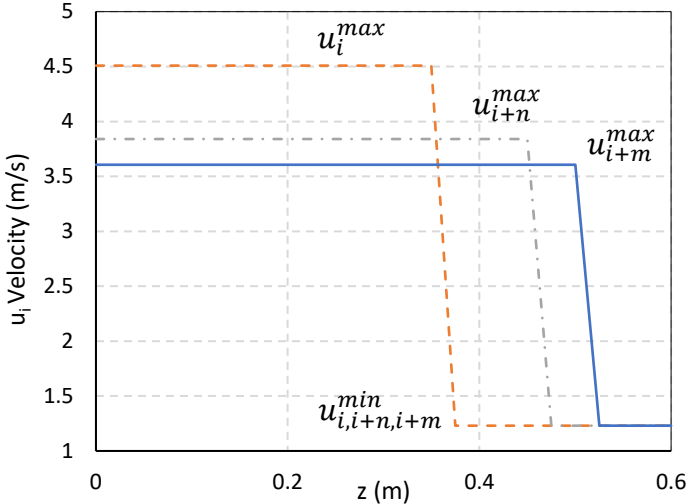
Figure 6. Inlet Velocity Profiles Examples

Three different heat rejections of 20, 40 and 80kW were presented. It could be observed that a higher imposed heat leads to a higher difference between 3D and 1D prediction. These phenomena can be seen in Figure 7. The resultant ΔT as a function of the UI linearly increases with increasing heat dissipation. Moreover, the effect of primary inlet profile minimal velocity is demonstrated in Figure 8. The graph shows that cases with an equal mass flow rate, heat dissipation (80kW) and inlet air profile uniformity could lead to different auxiliary (coolant) inlet temperature prediction. This is caused by the HTX domain characteristic heat dissipation Q-Table and the derivative nonlinear efficiency of heat transfer as a function of velocity. Thus, in the study the coolant inlet temperature depends on the step function minimal velocity magnitude.
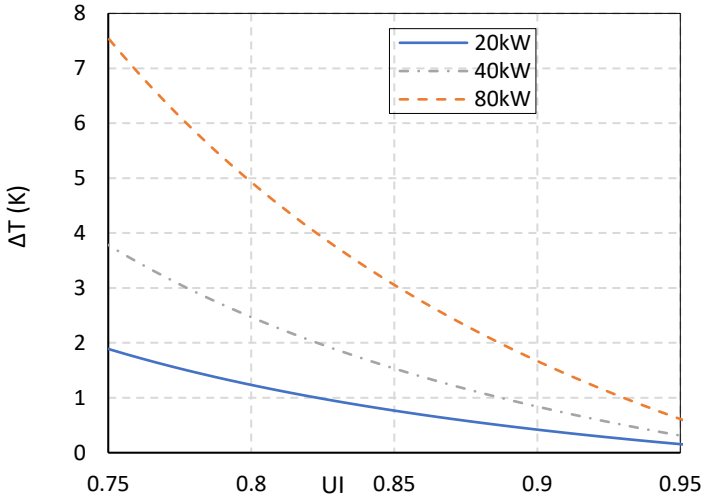
Figure 7. Heat Release Effect; Auxiliary Inlet Temperature as function of UI

8
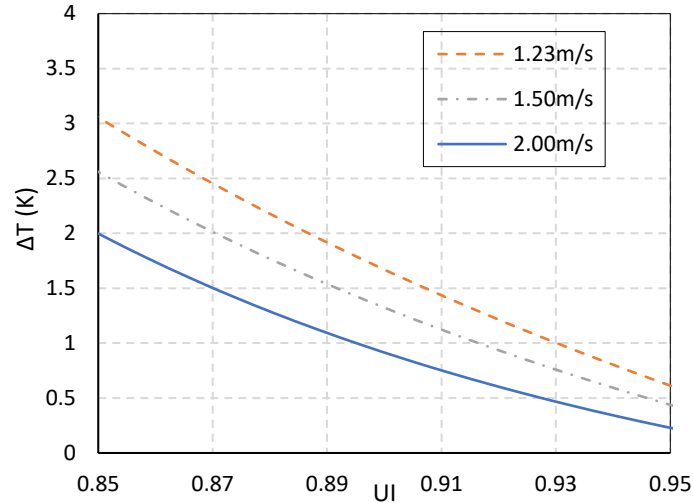
Figure 8. Air Inlet Velocity Effect; Auxiliary Inlet Temperature as function of UI

3. INDUSTRY APPLICATION

The industry data were used to verify the auxiliary inlet temperature is a function of air inlet profile also in industry application. The industry study was performed to confirm there is not a negligible difference between the 1D and 3D auxiliary fluid temperature prediction (ΔT). The full vehicle underhood thermal management 3D CFD simulation contains a huge number of components. The geometric complexity could lead to relatively lower values of the UI and low air inlet velocity regions and even stagnation regions, where the cooling air speed is close to zero. This phenomenon is common, especially for cases with small or zero vehicle speed. It should be noted that the air inlet temperature profile could also be very non-uniform as demonstrated in Figure 9 [20]. The figure shows a radiator cooling air inlet temperature profile as well as CAD of a underhood cooling pack to demonstrate the complexity of a common cooling pack as well. The air inlet temperature profile may be affected even by hot air recirculation or by the fact that the cooling pack consists of multiple heat exchangers, thus hot air passes through multiple HTXs. These effects are neglected within the presented work.

(a)　　　　　　　　　　　　　　　　　　　　(b)
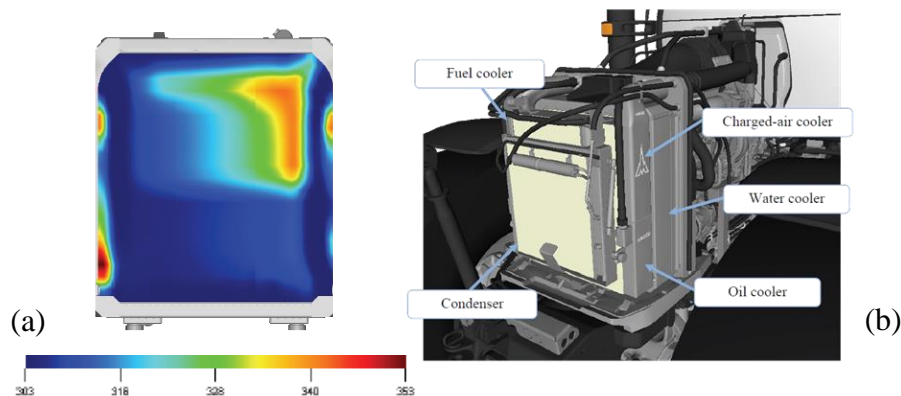
Figure 9 Real Vehicle Application - Temperature Profile (a) and Cooling Pack (b) **(19)**

The industrial application case used within the study is highlighted in Figure 10. The figure shows a vehicle cross-section in the longitudinal direction and a cooling pack inlet area air velocity magnitude contour. The full vehicle 3D CFD simulation was performed in the commercial tool Siemens STAR-CCM+. The raw results are not presented due to strictly

9

confidential content. However, the non-uniformity and complexity of the air flow pattern are sufficiently demonstrated within Figure 10. Furthermore, a section of the cooling pack inlet air flow velocity profile is applied into the HTX model to demonstrate 1D and 3D auxiliary fluid temperature prediction difference (ΔT) in industrial application. As the real vehicle HTX dimensions as well as discretisation of the full 3D UHTM simulation differ from the study HTX, a velocity magnitude mapping process is applied. The mapping process within the paper is defined as the distance weighted average from an appropriate surrounding area around an HTX study core computational node. In the expression **(13)**, the mapping technique and weighted function are demonstrated. The u_i refers to the study HTX core x direction velocity whereas the v_i signifies the full 3D underhood simulation velocity magnitude and the r is the radius of a circle in the area surrounding the node where the mapping search takes place.
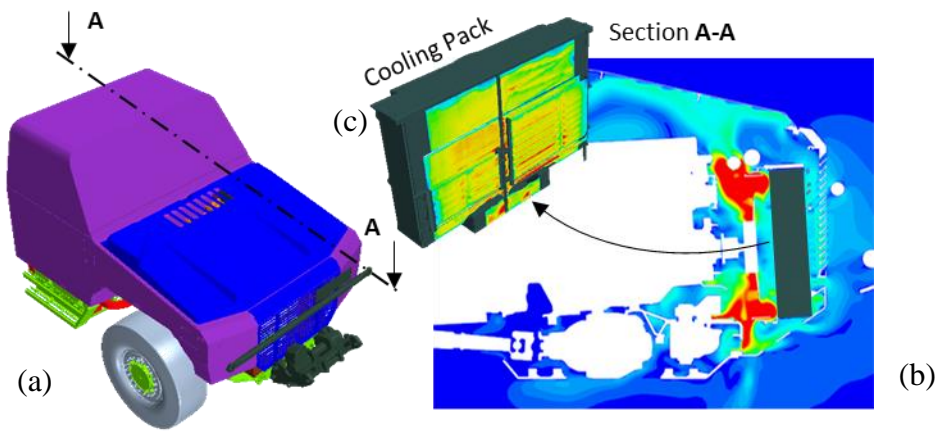
Figure 10. Real Vehicle Case – Vehicle Section (a), Air Flow (b) and Cooling Pack (c)

$$u_i = \frac{\sum v_i \cdot \omega_i}{\sum \omega_i} \qquad (11)$$

$$,where \ \omega_i = 1 - \left| \frac{\sqrt{(u_i^y - v_i^y)^2 + (u_i^z - v_i^z)^2}}{r} \right|$$

The calculation is defined with an uniform air inlet temperature of 306.43K and 80kW of dissipated heat. The rest of the material properties and coolant flow rate are the same as for the section of the Macro Based Model. It should be noted that the values are not completely identical with the full underhood vehicle model due to confidential data; however, the total values are not important for the conclusions. The resultant air inlet velocity profile as well as the computed air outlet temperature contour are shown in Figure 11.
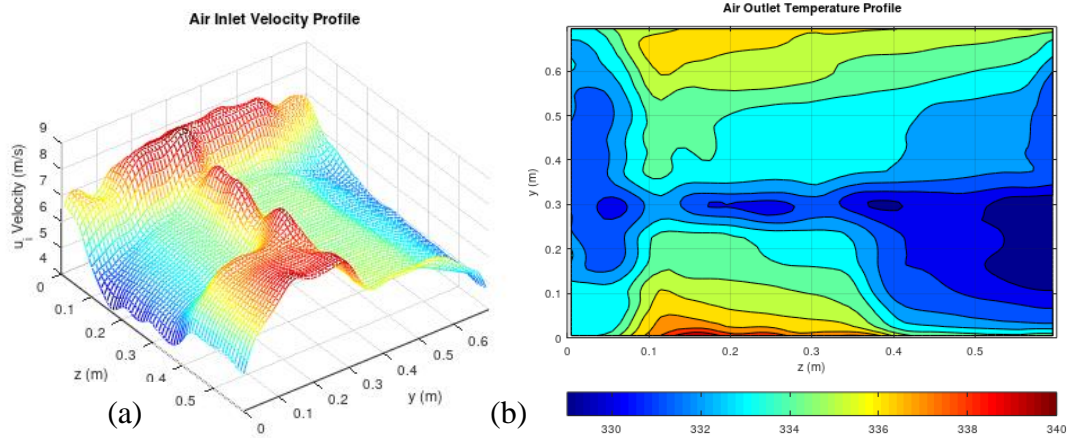
Figure 11. Applied Air Inlet Profile (a) and Predicted Air Outlet Temperature (b)

The resultant difference between the 1D and 3D coolant inlet prediction is 0.51K with the UI index of 0.94 and a minimal air inlet velocity of 4.06 m/s. This can be judged as feasible accuracy for typical industrial applications. However, once an artificial restriction is introduced into the air flow, the 1D underpredicts the coolant inlet temperature by 3.26K. The artificial restriction could represent a structural beam or other structural parts of the cooling pack, which is very likely for a modern vehicle. The second case with the restriction-section air inlet velocity as well as the air outlet temperature profiles are shown below in Figure 12. As a result of the air restriction, the UI is 0.90 lower in the second case compared to the first case without the restriction. Comparing the contour in Figure 11 and 12, it could be observed that the air outlet temperature is also affected outside the restriction region (higher air temperature). This reflects the coolant mixing after passing the HTX within the rest of the cooling circuit system (engine water jacket, pump, cabin heater etc.) and the steady-state conditions. The mixing is implemented in the solver via averaging the coolant inlet/outlet temperature whilst iterating and converging the HTX heat balance.
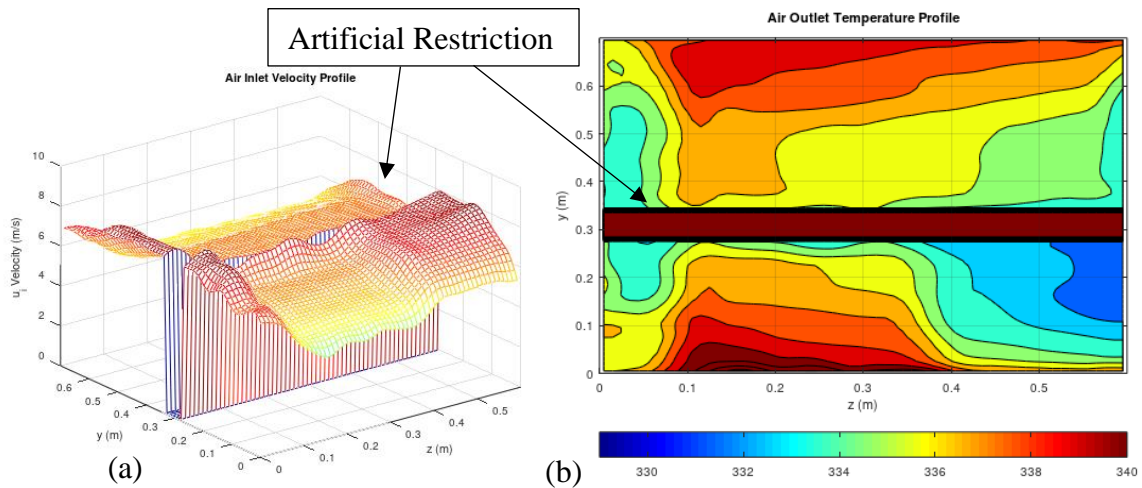
Figure 12. Applied Air Inlet Profile (a) and Predicted Air Outlet Temperature (b)

4. CONCLUSIONS

The evaluated heat exchanger (HTX) represents a typical vehicle single passed cross-flow type of HTX. The evaluated and analysed factor within the work is the scalar value of ΔT representing the difference in auxiliary fluid inlet temperature prediction between the 1D and 3D approaches. 1D refers to an approach assuming a uniform distribution of the primary fluid via the total mass flow rate or average inlet conditions in the case of a non-uniform inlet temperature profile. On the other hand, the 3D approach reflects the spatial distribution of primary fluid scalar values. Within the study, uniform primary (air) inlet temperature as well as constant material properties and zero pressure drop are assumed. These assumptions are feasible as the paper is focused only on the primary fluid inlet velocity spatial distribution effect on the auxiliary fluid flow inlet temperature prediction.

It has been confirmed that auxiliary fluid inlet temperature prediction is a function of primary fluid inlet velocity spatial distribution. The key factor affecting the ΔT identified during the work is the primary fluid inlet velocity uniformity index (UI). The impact of the UI effect linearly increases with heat dissipation in the HTX. An additional important factor is the quantitative characteristic of the primary fluid inlet flow profile, e.g. the velocity magnitude. Even with an equal mass flow rate and equal UI, the ΔT could differ between cases as was demonstrated by the results. However, these effects cannot be generalised as they are very case sensitive as HTX core heat transfer is a non-linear function of primary inlet velocity and HTX core behaviour differs between applications and HTX manufacturers.

The industrial example demonstrated the 1D approach which provides reasonably accurate results in a relatively uniform and high-speed velocity profile (Figure 11). However, it could lead to underpredicting auxiliary fluid flow inlet temperature in the case of relatively larger stagnating zones (Figure 12). Within the study, the stagnation region is represented with a local low airflow speed, which could be caused in the vehicle by the structural beam or other structural parts like holders, grill, etc. The scenario could lead, in the case of the 1D approach, to underpredicting auxiliary fluid flow inlet temperature. This could be crucial, especially in modern vehicles where the thermal management targets are very tight and a difference of a couple of degrees Celsius could lead to misleading conclusions, inefficient design changes, or not meeting a physical measurement target.

REFERENCES

[1]   Kim, H. J., Kim, C-J., 2008, "A numerical analysis for the cooling module related to automobile air-conditioning system," Applied Thermal Engineering, 28(14-15), pp. 1896-1905.

[2]   Mao, S., Feng, Z., Michaelides, E.E., 2010, "Off-highway heavy-duty truck under-hood thermal analysis," Applied Thermal Engineering, 30, pp. 1726-1733.

[3]   Ou, J. J., Li, L-F., Cui, T., Chens, Z-M., 2014, "Application of field synergy principle to analysis of flow field in underhood of LPG bus," Computers & Fluids, 103, pp. 186-192.

[4]   Binner, T., Reister, H., Weidmann, E. P., Wiedemann, J., 2006, "Aspects of Underhood Thermal Analyses"

[5]   Pang, S.C., Kalam, M.A., Masjuki, H.H., Badruddin, I.A., Ramli, R., Hazrat, M.A., 2012, "Underhood geometry modification and transient coolant temperature modelling for robust cooling networks," International Journal of Mechanical and Materials Engineering, 7, pp. 251-258.

[6]   Ding, W., Williams, J., Karanth, D., Sovani, S., 2006, "CFD Application in Automotive Front-End Design," SEA Technical Paper Series, Detroit.

[7]   Bolehovsky, O., Novotny, J., 2005, "Influence of underhood flow on engine cooling using 1-D and 3-D approach," Journal of Middle European Construction and Design of Cars, 13(3), pp.24-32.

[8]   Seider, G., Bet, F., 2013, "Flow and thermal performance prediction for automotive accessory units and their integration into underhood CFD flow analysis with multi thermal systems," Vehicle Thermal Management Conference Proceedings.

[9]   Saab, S., Hetet, J-F., Maiboom, A., Charbonnelle, F., 2013, "Impact of the Underhood Opening Area on the Drag Coefficient and the Thermal Performance of a Vehicle," SAE International,

[10]   Makam, S., Dubbs, C., Roosien, Y., Lin, F., Resh, W., 2015, "Analytical Study of Thermal Management: A Case Study of Underhood Configurations". SAE International.

[11] Vehovszky, B., Jakubík, T., Treszkai, M., 2019, "Thermal Examination of a Simplified Exhaust Tube-Heatshield Model," Periodica Polytechnica Transportation Engineering, 47(3), pp.190-195.

[12]   Shui-Chang, L., Li-Fu, L., Yong, Z., 2014, "Vehicle Radiators' Performance Calculation and Improvement Based on the Coupling Multi-scale Models Simulations," The Open Mechanical Engineering Journal, pp. 636-642.

[13]   Incropera, F. P. and DeWitt,. Fundamentals of Heat and Mass Transfer, 7th Ed., D. P. 2011, ISBN 13 978-0470-50197-9

[14]   Khot, A.R., Thombare, D.G., Gaikwad, S.P., Adadande, A.S. , 2013, "An Overview of Radiator Performance Evaulation and Testing". Journal of Mechanical and Civil engineering, pp. 07-14.

[15]   Navarro, H.A., Cabezas-Gomez, L.C., (2007), "Effectiveness-ntu computation with a mathematical model for cross-flow heat exchanger," Brazilian Journal of Chemical Engineering, 4,

[16]   ANSYS Fluent Theory Guide, release 12.0

[17]   Siemens STAR-CCM+ Theory Guide, release 13.04.010

[18]   SAE J902: Passenger Car Windshield Demisting and Defrosting Systems, 2011

[19]   S. Tischer, C. Correa, O. Deutschmann, 2001, "Transient three-dimensional simulations of a catalytic combustion monolith using detailed models for heterogeneous and homogenous reactions," Catalysis Today, 69, pp57-62.

[20]   Crippa, L., Mattei, M., Polidoro, F., Kleinclaus, C., Rousseau, Y., Xu, B., Alajbegovic, A., 2011, "Design and Analysis of Computer Experiments (DACE) and 3D Computation Fluid Dynamics (CFD) simulations for agricultural tractor cooling concept," pp. 459-471.